Monte Carlo Simulation and Well Testing Applied in Evaluating Reservoir Properties in a Deforming Longwall Overburden

Transport in Porous Media

ISSN 0169-3913
Volume 86
Number 2

Transp Porous Med (2010)
86:445-464
DOI 10.1007/
s11242-010-9628-2

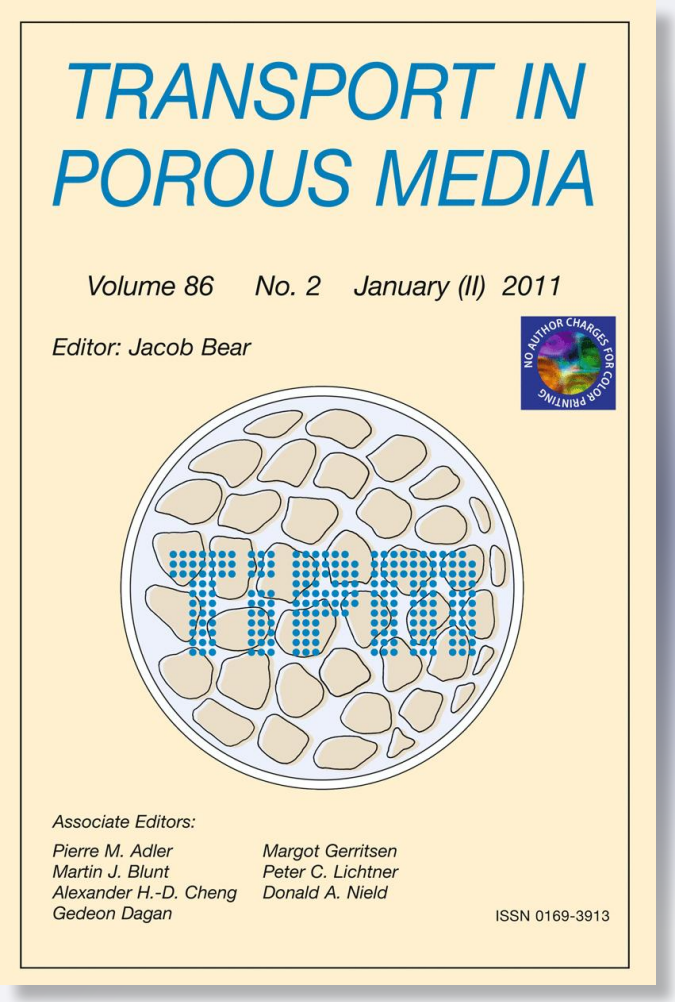

Springer

Transp Porous Med (2011) 86:445–464
DOI 10.1007/s11242-010-9628-2

Monte Carlo Simulation and Well Testing Applied in Evaluating Reservoir Properties in a Deforming Longwall Overburden

C. Özgen Karacan · Gerrit V. R. Goodman

Received: 12 February 2010 / Accepted: 19 July 2010 / Published online: 6 August 2010

Abstract During longwall mining, the intact strata start to deform and fracture as the mining face progresses. Gob gas ventholes (GGVs) are drilled from the surface over a longwall panel before mining to capture methane from the fractured zone. Due to fracturing and bedding-plane separations, reservoir properties change extensively. This poses a major problem for venthole designers and methane control engineers and may become a safety and health concern for underground work force due to unexpected methane emissions: it is difficult to predict the location of major strata separations and their temporal magnitudes to best locate the ventholes. Measurements obtained at different times during longwall mining may not be helpful for this purpose as strata deformation is a dynamic process and the results from different tests may not be lumped together to analyze the data collectively. This article uses a combination of Monte Carlo (MC) simulation and well testing methods to analyze multiple data sets obtained from a GGV at different longwall face locations. The aim was to determine the magnitude of average strata separation before conducting well test analyses to determine the properties of a deformed reservoir. MC simulation was used to process cross-correlated and uncertain data distributions obtained from measurements to generate a set of normally distributed values for each data type. These values were further used to project the amount of strata separation to the timing of well test. Finally, well-test analyses were used to interpret test data and to evaluate reservoir properties.

Keywords Reservoir · Gob gas venthole · Longwall gobs · Well testing · Monte Carlo method

List of Symbols

B_g Formation volume factor
c Compressibility (kPa^{-1}, psi^{-1})

C. Ö. Karacan (✉) · G. V. R. Goodman
NIOSH, Pittsburgh Research Laboratory, Pittsburgh, PA 15236, USA
e-mail: cok6@cdc.gov

h	Net pay (m, ft)
k	Permeability (md, md)
kh	Flow capacity (md.m, md.ft)
k/μ	Mobility
kh/μ	Transmissivity
P	Pressure (kPa, psia)
w	Channel thickness (m, ft)
q_j	jth flow rate (m^3/d, bbl/d)
q_n	nth flow rate (m^3/d, bbl/d)
r_e	External radius or radius of investigation (m, ft)
r_w	Wellbore radius (m, ft)
s	Apparent skin factor
t	Time (h, h)
t_a	Pseudo-time (h, h)
t_n	nth flow period or superposition time
Ψ	Pseudo-pressure for gas (kPa^2/Pa.s, $psia^2$/cp)

Subscripts

f	Formation or flowing
g	Gas
i	Initial
w	Wellbore

1 Introduction

1.1 Gob and Gob Gas Ventholes

Longwall mining is an extensive coal extraction process in a large area, called a "panel," above which the formation layers fracture and separate due to stress release and form a fractured zone called a "gob." Research in the Donetsk coal basin indicates that the thickness of the gob can vary up to 100 times the height of the mined coal seam, depending on the size of the panel and the geology and geomechanical properties of the layers (Palchik 2005).

The gob has high-permeability fractures that form easy pathways for gas transport towards the mining environment, making it of prime interest for gas control and production. Drilling vertical gob gas ventholes (GGVs), which only become productive as the longwall face advances under their locations, is an effective technique for capturing methane emissions within the overlying fractured strata before they enter the work environment.

1.2 Challenges in Gob and GGV Characterization

It is not always easy to characterize the fractured zone or to determine its reservoir properties. Measured data are scarce, and the dynamic nature of subsidence and associated changes adds complexity in conducting and evaluating tests. Tests must be conducted at the same time, since elapsed time between the tests will make interpreting results difficult. These challenges make it difficult to set up a numerical model of the gob for flow simulations. In turn, the challenges involved in testing, characterizing, modeling, and evaluating the reservoir properties of the gob also make it difficult to evaluate the performance and productivity of GGVs and to maintain underground health and safety in the face of high methane emissions.

Computational fluid dynamics (CFD) and techniques adapted from petroleum and gas engineering—such as reservoir simulation and well testing—can be useful in characterizing the gob reservoirs, simulating flow paths, and evaluating GGV performance, especially when they can be used in conjunction with rock mechanical models (Zuber 1998; Ren and Edwards 2002; Tomita et al. 2003; Karacan et al. 2007). Whittles et al. (2006, 2007) conducted studies on the effects of different geotechnical factors on gas sources and gas flow paths for British longwall operations, including how roof geology and its interactions with boreholes may cause the deformation and closure of the boreholes drilled for methane control.

Despite the improvements in modeling and understanding of GGV production performances, it is still difficult to accurately predict methane production from a GGV. Transient well test analysis methods, such as rate drawdown, interference, and pressure build-up tests, are developed for and applied in the petroleum and natural gas industry for both conventional reservoirs and coalbed methane reservoirs (Matthews and Russell 1967; Earlougher 1977; Dake 1978; Lee 1982; King et al. 1986; Mohaghegh and Ertekin 1991; Kuchuk and Onur 2003; Engler and Tiab 1996; Nashawi 2008; Kuchuk and Onur 2003; Valvatne et al. 2003; Escobar et al. 2007; Sheng 2009). These techniques can assist in understanding the characteristics of the gob reservoir and the interaction of GGVs with the gob and mining environment. However, the dynamic nature of the gob environment, changing reservoir properties, boundary conditions, and flow regimes make testing the reservoir and applying these techniques difficult without a priori analyses of all tests conducted.

1.3 Approach

Despite improvements in numerical modeling and testing techniques, the involvement of multiple influential factors and the unknowns related to strata fracturing and gas emission intervals continue to make evaluation of gob gas reservoirs and predictions about GGV performance difficult. Methane production from GGVs can often be characterized as an event with multiple episodic phenomena controlled by multiple variables associated with uncertainty and randomness. Therefore, deterministic methods of evaluation and their results may not always be satisfactory and they may need to be supported by stochastic methods, such as Monte Carlo (MC) methods. MC methods have been proven a useful tool for accurately estimating statistical uncertainties in standard errors and confidence intervals in nonlinear regression problems (Alper and Gelb 1990) as well as for studying groundwater flow and solute transport in heterogeneous, dual-porosity media (Huang et al. 2003).

This study used multi-rate drawdown test analyses and MC simulation to define the reservoir properties of the gob. Before setting up the well-test models, the magnitude of a major strata separation was determined using displacement measurements and flow measurements. Since there was time-lapse between well test and displacement measurement with formation markers, MC simulations were used to determine the amount of strata separations at a given time and to project it to well testing time.

2 Overview of the Data Collected from the Studied Gob Gas Venthole

2.1 Drilling and Completion of the Venthole

The GGV studied in this article was drilled to the top of the Sewickley coal bed (SWCB), approximately 82 ft above the Pittsburgh coal (PGH). The borehole was cased and cemented through the Waynesburg coal bed (WBCB). The bottom 254 ft of the borehole was left open,

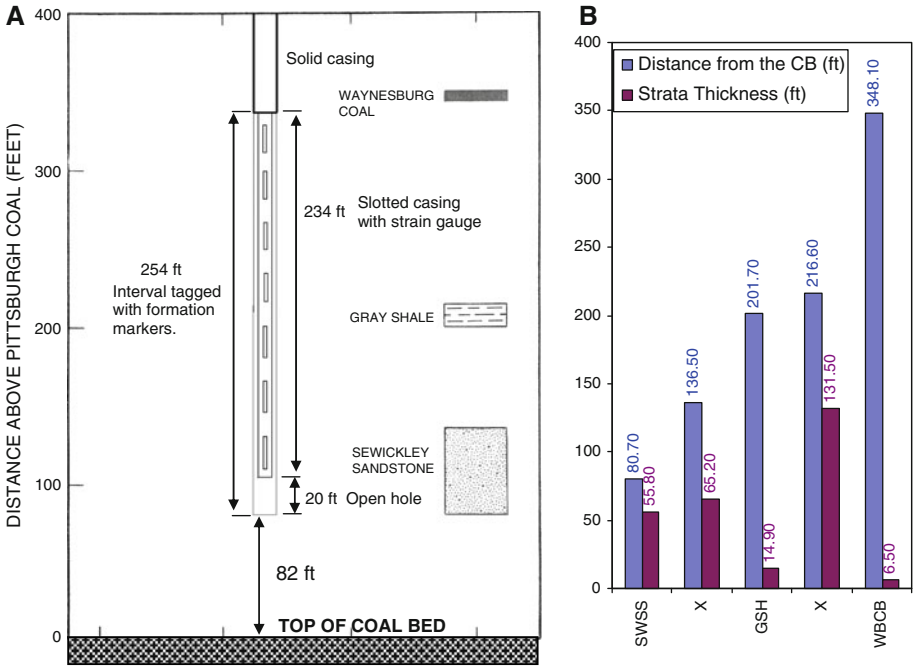

Fig. 1 The depth and completion details of the study GGV (**a**); the thicknesses of the major strata and their distances from the coal seam (**b**)

and this whole interval was tagged with radioactive formation markers. A strain gauge-equipped liner, with the bottom 234 ft slotted, was run to 20 ft above the total depth. The final 20 ft of the venthole was completed open hole (Fig. 1a). In this interval, Sewickley sandstone (SWSS) was 80.7 ft from the top of the PGH coal and was 55.8 ft in thickness (Fig. 1b). Gray shale (GSH), with a thickness of 14.9 ft, was 201.7 ft from the PGH coal. The interstitial sequences of shale and clay, marked as X in Fig. 1b, constituted a total of about 200 ft and were located from 136.5 and 216.6 ft from the PGH coal (Mazza and Mlinar 1977).

2.2 Initial Production of the Venthole

The venthole began production when the face was 58 ft past the venthole location (+58 ft), and the accumulated water was drained off. The krypton flow logger was used to determine points of flow entry when the face was +80 ft. At the time of this measurement, a total production flow rate of 109 scfm (157 msfcd) was recorded. Approximately, 85% of the flow entered in a 100-ft interval from the gray shale (GSH) formation to the Sewickley sandstone. The majority of flow entered the hole at the Sewickley sandstone horizon (Fig. 2b).

A gas sample taken shortly after the venthole began production contained 93% hydrocarbons and 5.7% carbon dioxide. The methane concentration remained above 90% until after the panel was completed. Produced gas was analyzed several times over the course of mining. Underground methane studies were conducted at various face positions. These measurements showed a 60% reduction in underground methane emission from 134 mscfd (93 scfm) before the venthole began production, to 55 mscfd (38 scfm) within the first week of venthole production (Table 1).

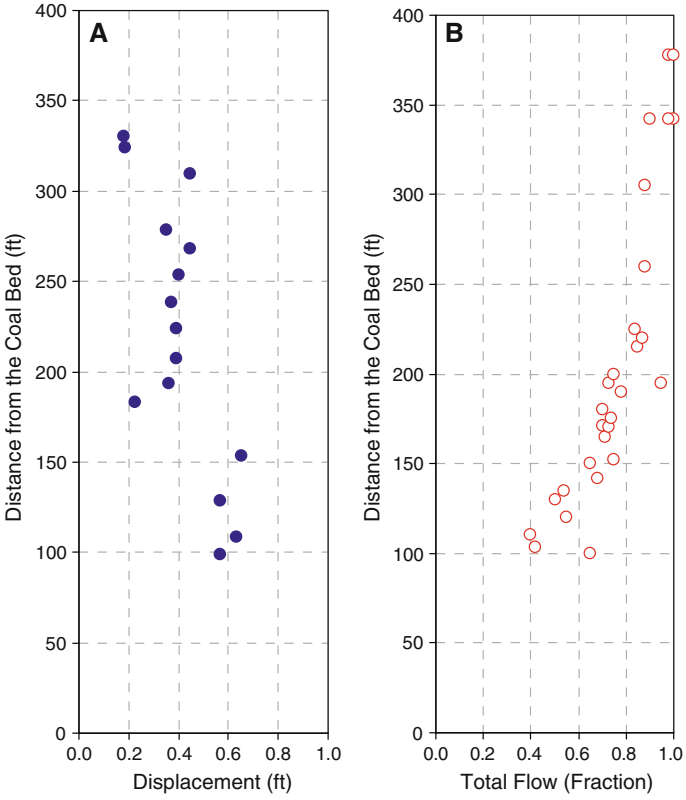

Fig. 2 Displacements (strata separations) measured using radioactive formation markers at +58 ft face location and percentage of total flow rate (157 mscfd) at +80 ft face location, using krypton data logger as a function of height from the coal bed. Displacement test (**a**); well test (**b**)

2.3 Strata Displacement and Casing Strains

On the initial day of production, when the face was +58 ft, a gamma ray survey was run to locate displacements. Strata separations of 0.2 ft occurred near the Waynesburg coal, 0.4 ft near gray shale, and 0.6 ft near the Sewickley sandstone (Fig. 2a). Although the strata separation was dependent on the location and the type of layer, the marker measurements along the length of casing resulted in an average displacement of 0.42 ft for the whole interval.

The slotted casing was equipped with a strain gauge (Fig. 1a), which enabled the measurement of loading at various face locations. The initial strain was mainly due to the weight of the casing and averaged 90.5 microstrains, which represented a load of 13,450 pounds. Casing strain began to increase rapidly once the face passed the venthole location. At +58 ft, the strain was 174 microstrains and at +95 ft it was 280 microstrains. The maximum casing strain of 454 microstrains occurred when the face was at +200 ft. As mining on the section continued and was finally completed, the casing strain settled down to a steady value of 226.9 microstrains (Fig. 3). This indicates that the casing was still under tension due to strata separation, and that some buckling might have occurred.

In order to characterize the whole strata of the venthole and to assign a single representative value for displacement, the average strata displacement of 0.42 ft, at a face location of

Table 1 Underground methane emissions and GGV production rates, and analyses of produced gas

Face position	Mine CH_4 emission rate (scfm)	GGV CH_4 prod. rate (scfm)	Total methane rate (scfm)	
Methane emission rate in the mine and methane production rate from the GGV				
+20 ft	93	0	93	
+64 ft	51	34.5	85.5	
+85 ft	38	80	118	
Gas	Test 1	Test 2	Test 3	Test 4
Analyses of the gas produced from the GGV				
CH_4	91.95	95.88	93.86	95.38
C_2H_6	0.84	0.8	0.73	0.73
C_3H_8	0.14	0.06	0.06	0.06
C_4H_{10}	0.02	–	–	–
CO_2	5.70	0.03	0.35	0.03
A	–	–	–	–
N_2	1.30	2.93	4.33	3.58
O_2	0.05	0.30	0.67	0.22
C_5H_{12}	–	–	–	–
N_2/O_2	26	9.77	6.46	16.27

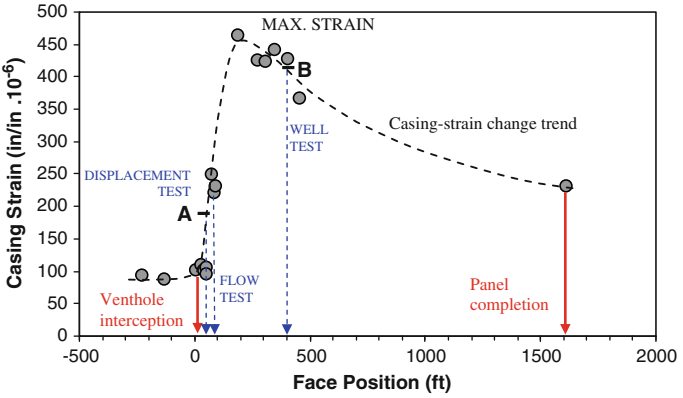

Fig. 3 Slotted casing strain measurements for the GGV, with locations of various tests

+58 ft, with a corresponding casing strain of 174 microstrains has been used. The average displacement value of 0.42 ft is also assigned to a depth of 175 ft from the top of the PGH coal, where the strata were potentially the weakest and most prone to separation (Fig. 2a).

2.4 Production Drawdown Tests for Venthole Productivity

A production drawdown test was conducted on the GGV to investigate production changes with time. The test determined production rate and wellhead pressure (Fig. 4) and was conducted with the longwall face at approximately +400 ft. The production rate had large changes, with small changes in wellhead pressure, indicating the infinite behavior of the gob

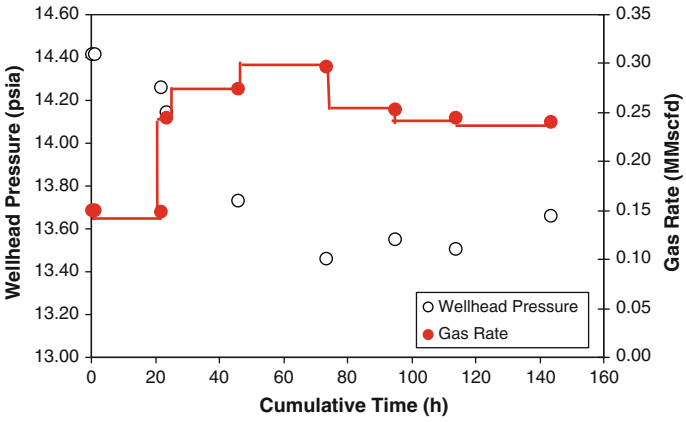

Fig. 4 Production drawdown test: gas rate and wellhead pressures as a function of time (+400 ft)

reservoir and the existence of high permeabilities. The latter is consistent with the observation of strata separations shown in Fig. 2.

The well-test data were used in conjunction with other measurements to evaluate the reservoir and its properties using rate drawdown test analyses. Different tests were conducted at different times and with the mining face at different locations with respect to the GGV (Fig. 3). This imposes different properties on the reservoir, as the reservoir was deforming during longwall face advance. In order to evaluate the well test data, it is important to determine the properties of the deforming formation at the time of the test.

2.5 Processing Data from Field Measurements

Since strata deformation, casing strains, face location, and subsequently measured flow fractions using krypton, data logging are correlated events and they carry uncertainty when projecting towards the time of well test, stochastic methods need to be used. Monte Carlo (MC) simulation was used to process cross-correlated distributions of measured data, their correlation matrix, and their means and standard deviations to generate a set of normally distributed values for each of the measured properties. These values were further used in MC simulation to project the amount of strata separation to the timing of well test. Finally, well-test analyses were used to interpret test data and to evaluate reservoir properties.

3 Evaluation and Analyses of the Data Measured from the Venthole

3.1 Stochastic Method (Monte Carlo) to Evaluate Measurements

In this study, the Monte Carlo method in RiskAMP (Structured Data 2008) was used to create multivariate normal distributions from measured data. Six univariate data sets were compiled from the field experiment. These data sets were fraction of total flow from the GGV, height above the coal seam measured during the flow test, strata displacement, height above the coal seam during the displacement test, casing strain, and longwall face location.

In order to generate multivariate normal distributions from univariate data, each of the data sets should be normally distributed (Krishnamoorty 2006). Therefore, each univariate data

Table 2 Calculated correlations between data sets, mean values, and standard deviations

	Face position	Casing strain	Displacement	Height from CB (1)	Flow fraction	Height from CB (2)	Mean	SD
Face position	1.00						173.27	154.04
Casing strain	0.85	1.00					268.47	150.17
Displacement	−0.50	−0.45	1.00				0.43	0.14
Height from CB (1)	0.93	0.88	−0.67	1.00			212.06	71.99
Flow fraction	0.87	0.82	−0.68	0.94	1.00		0.73	0.16
Height from CB (2)	0.93	0.78	−0.67	0.95	0.89	1.00	186.57	65.59

Height from CB (1) height from coal bed during displacement test, *Height from CB (2)* height from coal bed during flow test

set was first checked for normal distribution using a Q–Q plot, in which observed quantiles (the actual data) are plotted against calculated standard normal quantiles. If the data are from a normal population, the Q–Q plots will show an approximately linear relation. Correlations between the observed and standard quartile data in the Q–Q plots were calculated as 0.986, 0.949, 0.972, 0.997, 0.951, and 0.941 for total flow (in fraction), height above coal seam for total flow, displacement, height above coal seam for displacement, casing strain, and face location, respectively. These correlations are all greater than the critical values given in Looney and Gulledge (1985) indicating that the data are normally distributed and that they can be used in generating multivariate normal distributions.

Multivariate normal distributions were established using Monte Carlo simulations with the Cholesky decomposition technique (Clifford 1994) using RiskAMP (Structured Data 2008) with its "MultiNormalValue" function. The random number generation technique was Latin Hypercube. Application of MC for creating multivariate distributions generated a set of normally distributed numbers that retained the characteristics of the correlation matrix that result from the measured data and their means and standard deviations (Table 2).

During MC runs to generate multivariate distributions and numbers with normal distributions for each of the variables, the correlation matrix, means, and standard deviations were simulated by sampling data and trying to match both the correlation matrix of field measurements (observations) and their mean and standard deviation. These simulations were comparable to the observed values seen in Table 2. After 5,000 MC runs, the relative errors between the observations and simulations were equal to or less than 1%.

The values generated for each of the data sets and their frequencies are shown as normal distributions in Fig. 5. Figure 5a–f are histograms of the number of simulations as a function of calculated average values for face position (A), casing strain (B), displacement (C), height above coal seam for displacement measurements (D), fraction of flow (E), and height above coal seam for flow fraction measurement (F). These normal distributions that are shown in Fig. 5 address the multivariate nature of the data set to simulate the correlation matrix of observed data, means, and standard deviations discussed in the previous paragraph. The 5, 50, and 95% percentile values of the simulation results for all variables shown in Fig. 5 are given in Table 3.

From a fluid flow and transport point of view and to be able to interpret the well-test data, the most important parameter simulated in this study is the average value of strata displacement and its change from the time of its actual measurement (Fig. 3, point A: longwall face at +58 ft) to the time of the well test (Fig. 3, point B: longwall face at +400 ft). Casing strain

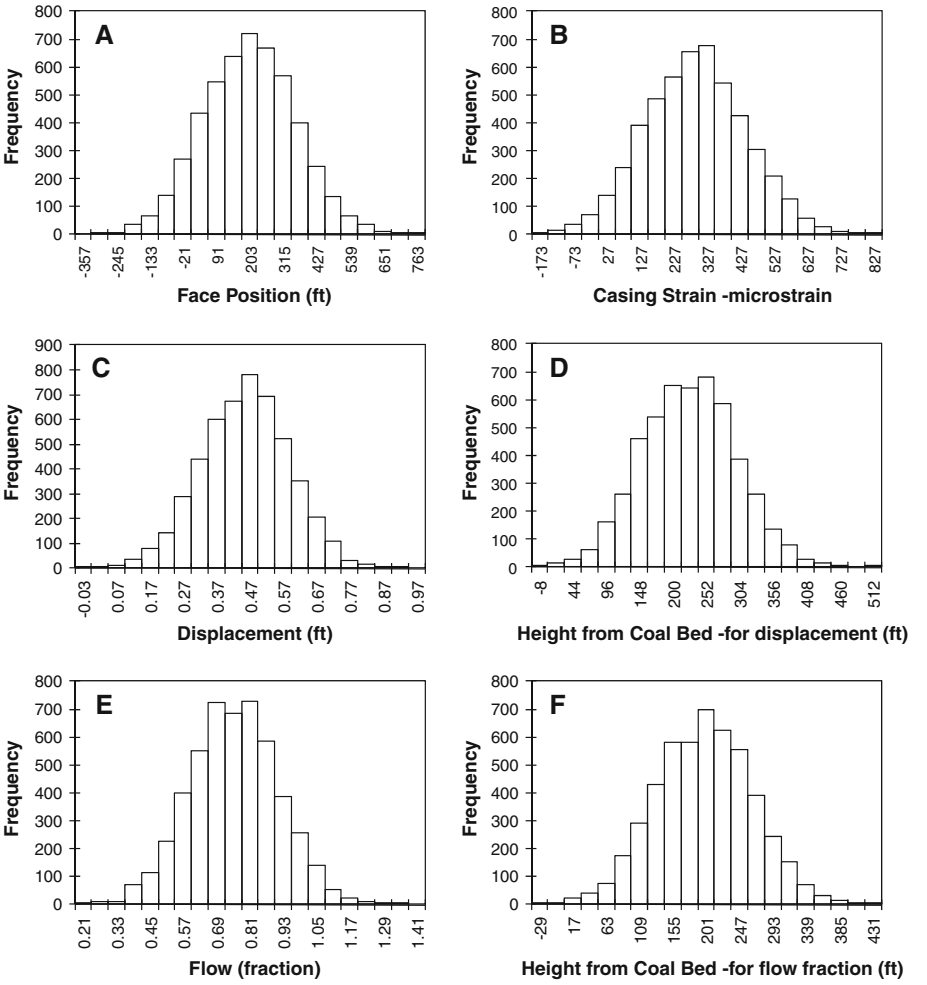

Fig. 5 Normal distributions (in frequency) of the field data generated using their mean and standard deviation in MC simulations

Table 3 5, 50, and 95% percentile values of MC simulation results

	5%	50%	95%
Face position	−77.41	173.67	425.50
Casing strain	19.73	270.69	512.91
Displacement	0.22	0.43	0.64
Height from CB (1)	92.60	212.77	326.02
Flow fraction	0.47	0.73	0.98
Height from CB (2)	76.63	186.05	291.67

is usually a good indicator of average vertical strata displacement, although strains can be created by horizontal displacements as well. Horizontal displacements will not be taken into account as they were not measured in this study. As Fig. 3 shows, casing strain is changing

Table 4 MC-determined mean values of the intercept and slope for linear relations between the data pairs

	Intercept	Slope	R^2
Face position–strain	125.8054	0.8272	0.73
Strain–average displacement	0.3556	0.0004	0.78

Table 5 Mean values for simulated strain and average displacements at +58 and +400 ft face positions

Face position (ft)	Strain (micro-strain)	Displacement (ft)
+58	173.8	0.43
+400	456.7	0.55

with the face location. Therefore, multivariate distributions generated for each variable using MC simulations were used to establish relations between average vertical displacements, casing strain, and face location for the changes from point A to point B in Fig. 3.

In order to generate a relationship between face position–strain and strain–average vertical displacement, only variable changes corresponding to points A and B in Fig. 3 were considered. This is equivalent to treating these variable pairs as state functions at A and B that can be determined based on the correlations within data, rather than path functions, which would have required known functional relationships. Therefore, the change in values of face position–strain and strain–average displacement between A and B can be represented with a linear function whose intercept and slope can be determined using MC simulations. The normal distributions of these parameter values are determined from all iterations of the simulation. Casing strain was selected as the dependent variable for face position–strain pair and average displacement was selected as the dependent parameter for the strain–average displacement pair. Table 4 gives the MC-determined mean values of the intercept and slope for these linear relations.

The MC-generated distributions and linear regression were used to calculate casing strain for face positions of +58 and +400 ft. Then, the newly obtained strain distributions and previously generated slope and intercept distributions were used to calculate values for the strain-average displacement pair. The mean values for simulated strain and displacements at +58 and +400 ft face positions are given in Table 5.

The predicted initial average displacement is 0.43, very close to the average displacement obtained from arithmetic average of measured values, 0.42. Table 5 also shows that the mean values calculated for strain at the time of the displacement test and well test are close to the arbitrary trendline shown in Fig. 3. This indicates that parameter distributions and their mean values can be predicted at any given point in a data set using MC simulations of multivariate correlations and distributions. As measured strain is caused by vertical displacements and bending and differential horizontal movements in the strata, it may always not be possible to find a one-to-one relation between strain and vertical displacement. This is one of the reasons why MC simulations were instrumental for evaluating face position–strain–vertical displacement data. The mean values show that casing strains increase as the longwall face advances past the GGV, illustrating the dynamic nature of strata changes and the deformation of the longwall gas reservoir during mining.

This study found that as the casing strain increased from ~175 to ~460 microstrains (1 microstrain: 10^{-6} ft extension of casing length per ft of original length), that change was accompanied with a mean simulated strata displacement, or fracture thickness, increasing from 0.43 to 0.55 ft as the face advanced from +58 to +400 ft. This value is used as the average thickness of the horizontal fracture at the time of the well test (+400 ft). As with

the measured average displacement value of 0.42 ft at +58 ft, this fracture is assigned to a height of 175 ft above the PGH coal.

4 Production Rate Drawdown Well Test Analysis of the GGV

4.1 Basic Considerations and Models

The production rate and wellhead pressure data (Fig. 4) that resulted from the rate drawdown are processed and analyzed using conventional well-test models. The models that are used in this study conceptualize the slotted casing section of the GGV in the form of three adjacent layers. The top layer (Z-1) and bottom layer (Z-3), which had 161 and 93 ft net pays, respectively, were modeled as dual-porosity formations to honor their natural fractures and minor bedding plane separations. These two layers were separated with a fracture layer (Z-2) of 0.55 ft net pay thickness, as estimated from MC simulations. The dual-porosity character of the top and bottom layers allowed them to have a fractured nature defined by ω and λ terms (storativity ratio and interporosity flow coefficient). Interporosity flow coefficient gives the permeability contrast between matrix and fracture with typical values of this coefficient between 10^{-4} and 10^{-8} in naturally fractured reservoirs. The storativity coefficient, on the other hand, is a measure of the fluid contained in the fractures and typically ranges between 10^{-2} and 10^{-1}. Lower values of the storativity coefficient means that most fluid is contained in the matrix. From a mechanistic point of view, reductions in the storativity coefficient denote longer periods of time for the matrix and fracture system to reach a state of equilibrium. The Z-2 layer was modeled as a homogeneous reservoir with 100% porosity.

The data were analyzed using linear-channel flow models. Linear-channel flow is a flow regime that exists in long, narrow reservoirs, and it occurs when the radius of investigation has reached the two closest parallel boundaries of the reservoir. The selection of this flow regime occurring in the layered and fractured strata of longwall overburden seems appropriate, given the nature of the problem, the characteristics of this reservoir, and considering a longwall panel as a long and narrow reservoir.

The models were analyzed by two different boundary conditions in the Z-1 and Z-3 layers: infinite and no-flow boundaries (Fig. 6a, b). Infinite boundaries were modeled because GGVs producing from a homogeneous-composite reservoir may experience infinite-reservoir boundary conditions as long as mining continues in the coal seam (Karacan 2009a). Continued longwall mining generates fracturing of the overlying strata which acts as an infinite source of gas to be produced by the operating GGV. As mentioned in Sect. 2.4, the large changes in production rate and small changes in wellhead pressure indicate that the gob reservoir in this study is behaving in an infinite manner. No-flow boundaries were modeled due to nature of the geometry of the panel and linear-channel flow regime.

Analyses of the data assumed a produced gas composition of 90% methane, 7% carbon dioxide, and 3% nitrogen. These values, based on the gas analyses shown in Table 1, were selected to be nearly representative of the four gas composition tests reported.

Interference effects from other wells can affect the analyzed pressure data during well testing in producing fields. Ideally, a multiple well simulation model should be used for analysis, using proper rate histories for each producer and accurate reservoir geometry. In this manner, the combined effects of neighboring wells can be added to the response of the tested well. However, different wells may not produce from the same layers, and the well spacing and the geometry of the reservoir boundaries may be difficult to describe with an analytical model. As a result, multiple-well simulation becomes very cumbersome and frequently

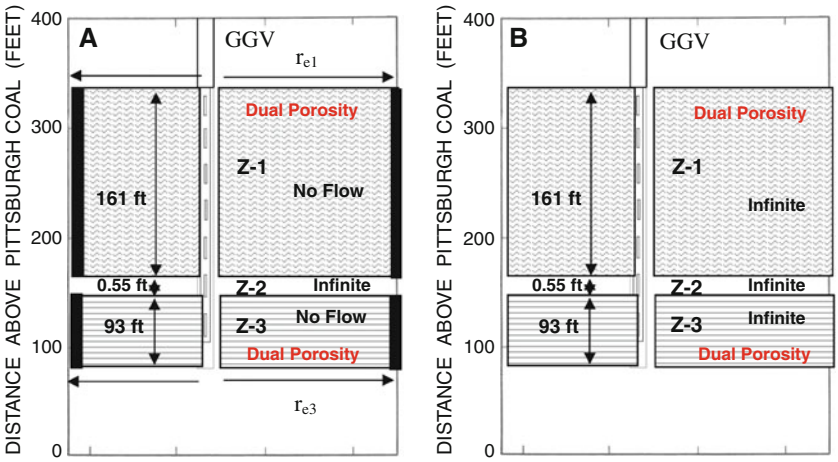

Fig. 6 Graphical representation of two models (**a** no-flow boundary conditions in layers Z-1 and Z-3; **b** infinite boundary conditions in all layers) used to analyze the well test data

many approximations have to be made. In many cases, tests are analyzed with a single-well-model approach (Bourdet 2003). Because of the complexity of the gob, a single-well-model approach was adopted in this study as well.

The wellbore storage term was considered "zero" in the analyses presented in this article. Usually, this term is needed when the compressibility of the wellbore fluid is not constant. Such situations may involve large drawdowns applied in gas wells or drastic changes in temperature in the borehole during production. At the study site, the GGV was relatively shallow and, thus, there was not much of a temperature gradient. Also, the surface blowers were applying small suction pressures for gas production. Therefore, wellbore storage effects could safely be neglected under these circumstances.

In this study, the gas flow rates and the flowing pressures at the wellhead of the GGV (Fig. 4) were evaluated using multi-rate drawdown gas well testing methods. With such analyses, wells should ideally produce at a constant rate to reach stabilized flow conditions after a rate change. Since the permeability of gob reservoirs is usually very high, the reservoir can attain stabilized flow conditions almost instantly, making application of multi-rate drawdown tests easier.

In the well-test analysis, F.A.S.T. WellTest (Fekete Associates 2009) software was used to evaluate total gas production and wellhead pressure data obtained during testing. In order to model the data for parameter search and optimization, the automated parameter estimation (APE) with Simplex algorithm was used.

4.2 Brief Theory of the Well Test Analysis Techniques Used for the Production Data of this Study

This study uses multilayer cylindrical models to evaluate the well-test data in a heterogeneous and layered reservoir (Fig. 6). The multilayer model simulates the flow in a number of independent layers commingled at the wellbore. Each layer has a cylindrical geometry with an identical initial pressure and can have its own skin factor and reservoir properties, such as dual-porosity, as well as its own outer boundary conditions. In the solution of the multilayer model, equations are solved in the Laplace domain, and then inverted to the real-time domain

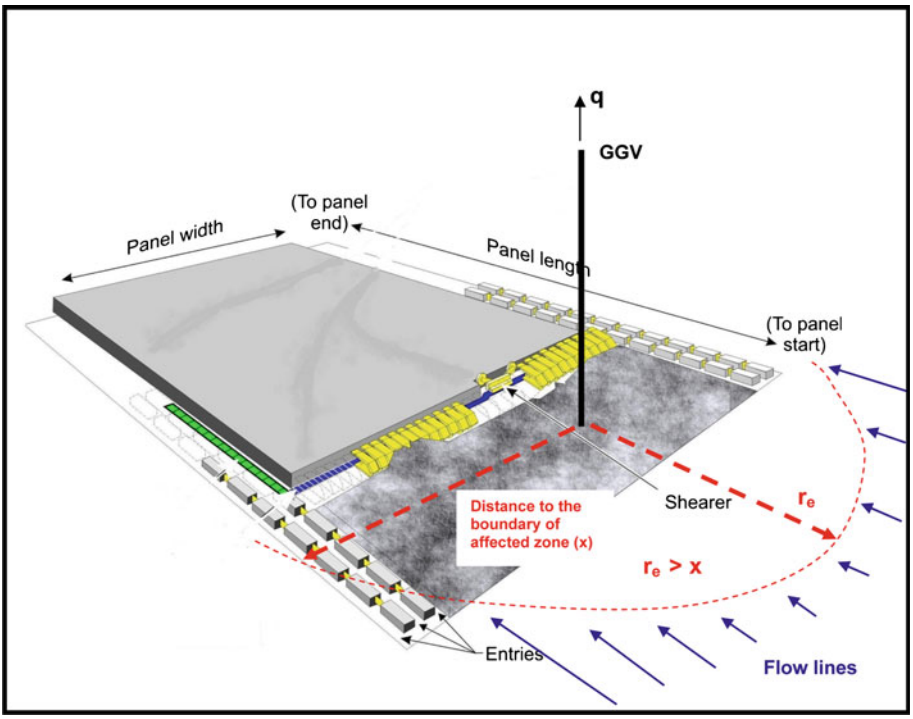

Fig. 7 Schematics of a longwall panel and linear channel flow regime that may develop during production of a GGV and how it relates to panel geometry and the size of the affected area

by using the Stehfest algorithm. The result is superposed in time according to the schedule of rates input in the production history (Fekete Associates 2009).

Linear channel flow occurs in long, narrow reservoirs. Before the radius of investigation reaches the reservoir boundaries, radial flow is observed. After the two parallel boundaries are reached, a period of linear channel flow can be observed. The linear channel flow regime that may develop during GGV production is related to the longwall panel environment of the particular GGV (Fig. 7).

The constant rate solution for rate-drawdown test for analyzing linear channel flow is (Fekete Associates 2009):

$$\psi_{\mathrm{wf}}(t) = \psi_i - 8.157 \times 10^4 \frac{q_{\mathrm{g}} T}{hW} \frac{\sqrt{t_{\mathrm{a}}}}{\sqrt{k\phi\mu_{\mathrm{gi}} c_{t_i}}} \tag{1}$$

where ψ is the real-gas pseudo pressure that is used in place of pressure in natural gas engineering. It is defined as:

$$\psi(p) = 2 \int_{p_b}^{p} \frac{p dp}{\mu Z} \tag{2}$$

Linear channel flow data will form a straight line when $\frac{\Delta\psi}{q}$ is plotted versus $\sqrt{t}$ in a linear plot. The slope of this line can further be used to determine W (channel thickness):

$$W\sqrt{k} = \frac{8.157 \times 10^4 T}{\text{slope} \times h\sqrt{\phi\mu_{\text{gi}}c_{\text{ti}}}} \tag{3}$$

The derivative of (1) with respect to natural logarithm of time is:

$$\text{Der} = \frac{1}{2}8.157 \times 10^4 \frac{q_{\text{g}}T}{hW}\frac{1}{\sqrt{k\phi\mu_{\text{gi}}c_{\text{ti}}}}\sqrt{t_{\text{a}}} \tag{4}$$

Taking the logarithm of both sides of (4) gives:

$$\log(\text{Der}) = \log\left(\frac{1}{2}8.157 \times 10^4 \frac{q_{\text{g}}\mu B}{hW}\frac{1}{\sqrt{k\phi\mu c_t}} + \frac{1}{2}\log t\right) \tag{5}$$

Resulting in a slope of $(\frac{1}{2})$ when plotted $\log(\frac{\Delta\psi}{q})$ versus $\log(t_{\text{a}})$-diagnostic plot from:

$$\frac{1}{2}8.157 \times 10^4 \frac{T}{h\sqrt{\phi\mu_{\text{gi}}c_{\text{ti}}}}\frac{\sqrt{t_{\text{a}}}}{\text{Der}} \tag{6}$$

4.3 Superposition in Time

In order to apply the presented equations (1–6) and techniques for multi-rate production histories, the "elapsed time" should be defined using the superposition theorem. This theorem mathematically states that any sum of individual solutions of a second-order linear differential equation is also a solution of the equation itself (Dake 1978). Thus, superposition in time for a well producing with multiple rate conditions for various durations means that individual constant rate wells can be placed in the same position in the reservoir at any time and that an expression for the resulting pressure distribution in time can be derived (Dake 1978). The superposition time used in this study to analyze the data was:

$$t_n = \sum_{j=1}^{n} \frac{q_j - q_{j-1}}{q_n}\log(t - t_{j-1}) \tag{7}$$

$$\Delta t_n = \sum_{j=1}^{n} \frac{q_j}{q_n}\log\frac{t_n + \Delta t - t_{j-1}}{t_n + \Delta t - t_j} \tag{8}$$

4.4 Analyses of Test Data and Results

Before starting the analysis of data using multilayer models to determine reservoir parameters, a diagnostic plot was performed. A diagnostic plot is simply the plot of $\log(\frac{\Delta\psi}{q})$ versus $\log(t_{\text{a}})$ of the test data, overlaid with the characteristic shapes of different models to see which shape best represents the data. This allows selection of the appropriate theoretical model. The diagnostic plot for the present data best matches the 1/2-slope line which is characteristic of linear channel flow (Fig. 8).

The graphical results obtained from analyses on the two multilayer models are shown in Fig. 9 (no-flow boundary model; Fig. 6a) and Fig. 10 (infinite boundary model; Fig. 6b).

Figure 9a–d shows the results for the case where layers Z-1 and Z-3 had no-flow boundaries (Fig. 6a). Figure 10a–d, on the other hand, shows the results where all layers had infinite reservoir boundaries (Fig. 6b). In these figures, the A plot is the match of observed wellhead pressures with the model predictions and the matching errors. These figures show that

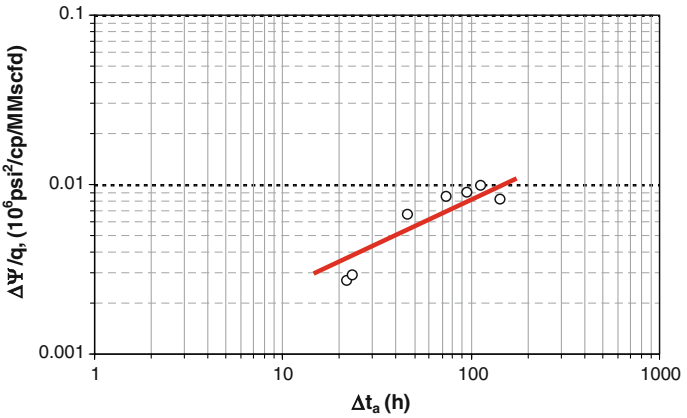

Fig. 8 Diagnostic plot of test data, overlaid with 1/2 slope line characteristic of linear channel flow

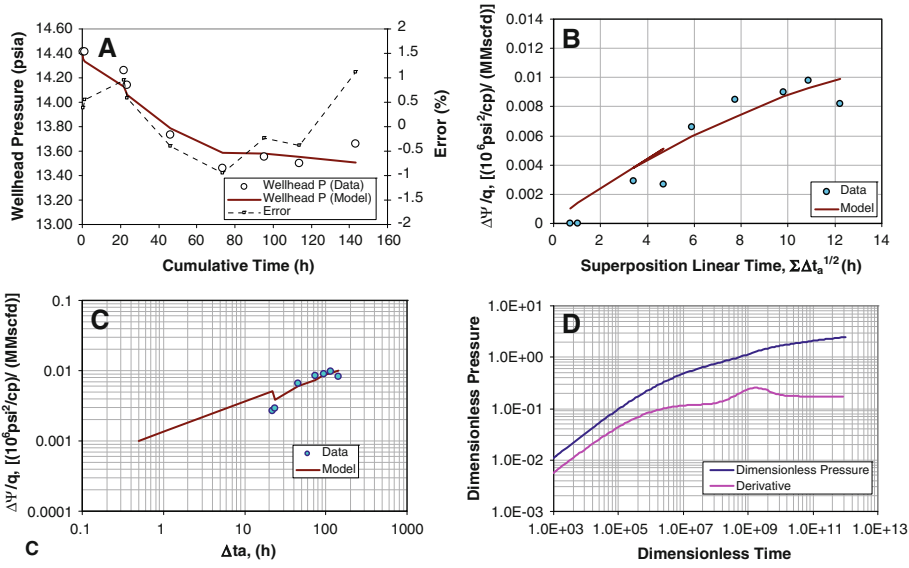

Fig. 9 Graphical results obtained from analyzing data with the multilayer model shown in Fig. 6a

model-matching errors were less than ±1%. Figures 9b and 10b are predictions to data that were plotted as $\frac{\Delta\psi}{q}$ versus $\sqrt{t}$. This data show that models generated nearly straight lines, which was expected from linear channel flow analyses where such slopes can be used for parameter estimations. Figures 9c and 10c are curve fits of model predictions to data when plotted on a log–log plot. Finally, D plots in each figure are the dimensionless type curves that are predicted by the model based on the system behavior. The term type-curve refers to a log–log plot of a specific solution to a flow equation (Ramey 1970).

From a qualitative point of view, all of the plots for the model with no-flow boundaries are very similar to their counterparts with infinite boundaries. Even the errors shown in Figs. 9a and 10a are of the same magnitude. The only noticeable difference is the "hump" in the derivative plot of the dimensionless pressure–time curve in Fig. 9d. The effect of dual-porosity

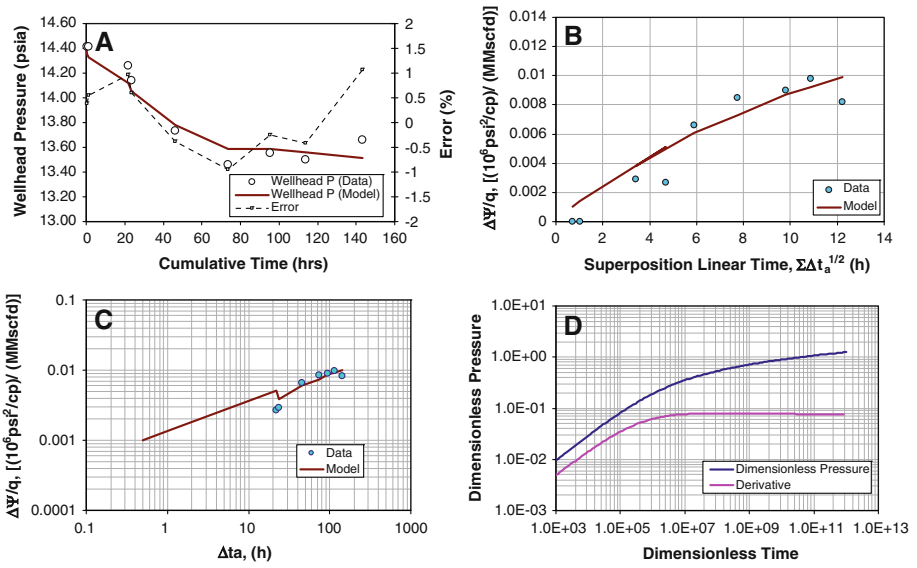

Fig. 10 Graphical results obtained from analyzing data with the multilayer model shown in Fig. 6b

behavior is usually characterized by the inverse of a hump, a "dip" (Horne 1990). An observed hump may be a boundary effect, related to pressure transients reaching the no-flow boundaries in the Z-1 and Z-3 layers. Nevertheless, the qualitative similarities and interpretations of these plots of model may indicate that the boundary conditions imposed on layers Z-1 and Z-3 have minimal effects on the overall reservoir behavior and the rate-pressure history of the GGV. This may also indicate that the fracture layer is the main layer controlling system behavior.

The reservoir parameters calculated from the plots can be seen in Table 6. The highest permeability layer is the Z-2 fracture layer, adding weight to the notion of the fracture layer controlling the reservoir behavior. It has permeability on the order of 140–160 Darcies. These values are consistent with the permeability of fractures calculated from geomechanical models and used in reservoir simulation studies of gobs (Karacan et al. 2007).

By comparison, the permeability values calculated for Z-1 and Z-3 are in the range of 100–250 md, about three orders of magnitude lower than the major strata fracture modeled at Z-2. These values are indicative of natural fractures or minor strata separations. Due to these relatively low permeabilities, the flow capacities (kh) calculated for Z-1 and Z-3 are about 3–4 times less than the flow capacity of Z-2, despite its small thickness. These results are consistent with field measurements and calculations that indicate that most of the gas from GGVs is produced within major strata separations or tension fractures. This implies that for high methane productivity and effective methane control, locating the GGV slotted casings at the height of major fractures is extremely important. Further, this shows the importance of calculating the most probable thickness of the fracture layer in deforming strata using all sources of information and techniques such as MC. If the most probable thickness of this fracture had not been estimated for the time of the well test, the permeabilities would have been over- or underestimated (assuming flow capacities would stay the same).

The apparent skin values (s) calculated for all layers of the models have negative values. Negative skins are indicative of stimulation in the wellbore, such as fracturing. The more

Table 6 Reservoir parameters calculated for the multilayer models

	Z-1	Z-2	Z-3
Model: Fig. 6a			
kh (md.ft)	26570.4	77746.2	23214.6
h (ft)	161.0	0.55	93.0
k (md)	165.03	141356	249.62
s	−1.226	−8.861	−2.515
r_e (ft)	4214.8	–	3916.2
ω	0.008	–	0.004
λ	2.35×10^{-7}	–	2.86×10^{-8}
Model: Fig. 6b			
kh (md.ft)	18221.0	86112.6	18727.3
h (ft)	161.0	0.55	93.0
k (md)	113.17	156568	201.37
s	−2.046	−8.755	−3.727
r_e (ft)	–	–	–
ω	0.016	–	0.01
λ	7.65×10^{-7}	–	3.09×10^{-8}

negative the number, the more the formation may be fractured. Z-2 has a skin value of nearly −9, compared to −1 to −3 in Z-1 and Z-3, which is consistent with the permeabilities calculated for these layers. Z-3 has a more negative skin than Z-1, which is consistent with its higher permeability compared to Z-1.

For the no-flow boundary model, the radii of investigations (r_e) were also determined for Z-1 and Z-3. These values showed that Z-1 had a radius of ∼4200 ft, whereas Z-3 had a radius of ∼3900 ft. These are the minimum distances beyond which any event would not be observed during the test period. However, due to the averaging effects of the results, the complete reservoir area affected by the well production may be confined in a different circular area around the wellbore (Oliver 1990). The calculated radius of investigation from the well tests gives an approximate value and an order of magnitude idea about the true distance for the existence of boundaries, rather than an exact distance. With this information and with the observation that the placement of boundaries in the no-flow model did not affect the results appreciably, it can be argued that in this test, the calculated boundaries were far enough removed from the wellbore that they acted as if they were infinite.

Finally, Table 6 gives the interporosity flow (λ) and storativity (ω) coefficients due to the dual porosity nature of Z-1 and Z-3. Interporosity flow coefficients are on the order of 10^{-7} to 10^{-8}, which is within the expected range of 10^{-4} to 10^{-8}. However, having interporosity flow coefficients close to the low end of the range indicates that fracture permeabilities for those layers are much higher compared to the matrix permeabilities. This makes sense, as the geologic layers in those model intervals are mostly shales, clay and mudstones (Karacan 2009b) with no or very little matrix permeability. Similarly, calculated values for the storativity coefficient are on the order of 0.01 and less, indicating that matrices in those layers host more fluid compared to the fractures.

5 Summary and Conclusions

Gob gas ventholes are one of the primary measures of controlling excessive methane emissions from surface before they enter the underground coal mines and create a threat to safety. This article illustrates the use of Monte Carlo simulation and well-testing methods to assess methane reservoir properties using the production characteristics of a GGV drilled above a longwall gob. Drilling and subsequent testing of the GGV showed initial methane production began shortly after the longwall face passed beneath the venthole. Gamma ray logging revealed the presence of distinct strata separations near the Waynesburg coal, near the gray shale beneath the Waynesburg coal, and near the Sewickley sandstone layer. Average strains on the well casing were measured and shown to increase rapidly as the face undermined the borehole location. Gas productions varied with wellhead pressures, suggesting the presence of high permeability pathways in the gob reservoir.

In order to assess reservoir properties of the deforming gob, Monte Carlo simulation was used to transform the acquired field data of fraction of total flow from the GGV, height above the coal seam during flow test, strata displacement, height above the coal seam during displacement test, casing strain, and longwall face location into multivariate normal distributions. After 5,000 iterations in the Monte Carlo simulations, differences between observed and simulated values were $\leq 1\%$. Multivariate distributions established the covariance between different measurements. Monte Carlo simulation was further used to project the measured quantities from different tests performed at different times to a common temporal position. In this process, relations between face position and casing strain, and casing strain and strata displacement, were established. This procedure quantified the strata separations when the longwall face was 58 and 400 ft past the borehole. Results from the simulation indicate that strata separation at the time of rate drawdown test (face at 400 ft past the borehole location) was 0.55 ft, which was later used as the fracture thickness when analyzing the production rate and well head pressure data obtained during the well test.

Well-test analyses of the data assumed the presence of three distinct and adjacent gas producing layers within the GGV. The gas flow within the top and bottom layers was modeled assuming either no-flow or infinite boundary conditions, while gas flow within the middle layer was modeled as an infinite reservoir. These analyses further assumed a dual porosity formulation for the top and bottom layers and a homogenous formulation for the middle layer. Model results for no-flow conditions were very similar to those obtained for the infinite boundary conditions. These outputs suggested that the boundary conditions imposed on the top and bottom layers had minimal impact on the behavior of the gob reservoir and that the middle layer may, in fact, have been the factor that most controlled the production potential of the gob. The results also revealed that permeability of the middle layer was roughly three orders of magnitude higher than those calculated for the top and bottom layers indicating major strata separation within the middle layer. These data suggest the importance of locating the slotted casing within these major strata separations, as well as quantifying the thickness of major strata separations using methods such as Monte Carlo, as these separations are the major conduits for flow.

References

Alper, J.S., Gelb, R.I.: Standard errors and confidence intervals in nonlinear regression: comparison of Monte Carlo and parametric statistics. J. Phys. Chem. **94**, 4747–4751 (1990)

Bourdet, D.: Practical aspects of well-test interpretation. In: Cubitt, J. (ed.) Handbook of Petroleum Exploration and Production, pp. 351–375. Elsevier, Amsterdam (2003)

Clifford, P.: Monte Carlo methods. In: Stanford, J.L., Vandeman, S.B. (eds.) Methods of Experimental Physics, vol. 28, pp. 125–153. Academic Press, London (1994)
Dake, L.P.: Fundamentals of Reservoir Engineering, 443 pp. Elsevier, Amsterdam (1978)
Earlougher, R.C.: Advances in Well Testing, 264 pp. Society of Petroleum Engineers of AIME, Dallas, TX (1977)
Engler, T., Tiab, D.: Analysis of pressure and pressure derivative without type curve matching, 4. Naturally fractured reservoirs. J. Petrol. Sci. Eng. **15**, 127–138 (1996)
Escobar, F.H., Ibagon, O.E., Montealegre, M.M.: Average reservoir pressure determination for homogeneous and naturally fractured formations from multi-rate testing with the TDS technique. J. Petrol. Sci. Eng. **99**, 204–212 (2007)
Fekete Associates.: F.A.S.T. WellTest v. 7.1.1. http://www.fekete.com/software/welltest/description.asp (2009)
Horne, R.N.: Modern Well Test Analysis. pp. 183 Petroway Inc., Palo Alto, CA (1990)
Huang, H., Hassan, A.E., Hu, B.X.: Monte Carlo study of conservative transport in heterogeneous dual-porosity media. J. Hydrol. **275**, 229–241 (2003)
Karacan, C.Ö.: Reconciling longwall gob gas reservoirs and venthole production performances using multiple rate drawdown well test analysis. Int. J. Coal Geol. **80**, 181–195 (2009a)
Karacan, C.Ö.: Reservoir rock properties of coal measure strata of the Lower Monongahela Group, Greene County (Southwestern Pennsylvania), from methane control and production perspectives. Int. J. Coal Geol. **78**, 47–64 (2009b)
Karacan, C.Ö., Esterhuizen, G.S., Schatzel, S.J., Diamond, W.P.: Reservoir simulation-based modeling for characterizing longwall methane emissions and gob gas venthole production. Int. J. Coal Geol. **71**, 225–245 (2007)
King, G.R., Ertekin, T., Schwerer, F.C.: Numerical simulation of the transient behavior of coal-seam degasification wells. SPE Form. Eval. **1**, 165–183 (1986)
Krishnamoorty, K.: Handbook of Statistical Distributions with Applications. pp. 346 Chapman and Hall/CRC, Boca Raton, FL (2006)
Kuchuk, F.J., Onur, M.: Estimating permeability distribution from 3D interval pressure transient tests. J. Petrol. Sci. Eng. **39**, 5–27 (2003)
Lee, J.: Well Testing, 159 pp. Society of Petroleum Engineers of AIME, Dallas, TX (1982)
Looney, S.W., Gulledge, T.R. Jr.: Use of the correlation coefficient with normal probability plots. Am. Stat. **39**, 75–79 (1985)
Matthews, C.S., Russell, D.G.: Pressure Buildup and Flow Tests in Wells, 172 pp. Society of Petroleum Engineers of AIME, Dallas, TX (1967)
Mazza, R.L., Mlinar, M.P.: Reducing methane in coal mine gob areas with vertical boreholes. U.S. Department of the Interior, Bureau of Mines, Research Report No. 1607-1-77, Pittsburgh, PA (1977)
Mohaghegh, S., Ertekin, T.: A type-curve solution for coal seam degasification wells producing under two-phase flow conditions. In: Proceedings of 66th Annual Technical Conference and Exhibition of Society of Petroleum Engineers, Dallas, TX (1991)
Nashawi, I.S.: Pressure transient analysis of infinite-conductivity fractured wells producing at high flow rates. J. Petrol. Sci. Eng. **63**, 73–83 (2008)
Oliver, D.S.: The averaging process in permeability estimation from well-test data. SPE Form. Eval. **5**, 319–324 (1990)
Palchik, V.: Locatization of mining-induced horizontal fractures along rock layer interfaces in overburden: field measurements and prediction. Environ. Geol. **48**, 68–80 (2005)
Ramey, H.J. Jr..: Short-time well test data interpretation in the presence of skin effect and wellbore storage. J. Petrol. Technol. **22**, 97–104 (1970)
Ren, T.X., Edwards, J.S.: Goaf gas modeling techniques to maximize methane capture from surface gob wells. In: De Sauza, E. (ed.) Mine Ventilation, pp. 279–286. Swets and Zeitlinger B.V., Lisse, The Netherlands (2002)
Structured Data: RiskAMP: Risk Analysis and Modeling Program. www.riskamp.com (2008)
Sheng, J.J.: A new technique to determine horizontal and vertical permeabilities from the time-delayed response of a vertical interference test. Transp. Porous Media **77**, 507–527 (2009)
Tomita, S., Deguchi, G., Matsuyama, S., Li, H., Kawahara, H.: Development of a simulation program to predict gas emission based on 3D stress analysis. In: 30th International Conference of Safety in Mines Research Institutes, South African Institute of Mining and Metallurgy, pp. 69-76 (2003)
Valvatne, P.H., Serve, J., Durlofsky, L.J., Aziz, K.: Efficient modeling of nonconventional wells with downhole inflow control devices. J. Petrol. Sci. Eng. **39**, 99–116 (2003)
Whittles, D.N., Lowndes, I.S., Kingman, S.W., Yates, C., Jobling, S.: Influence of geotechnical factors on gas flow experienced in a UK longwall coal mine panel. Int. J. Rock. Mech. Min. Sci. **43**, 369–387 (2006)

Whittles, D.N., Lowndes, I.S., Kingman, S.W., Yates, C., Jobling, S.: The stability of methane capture boreholes around a longwall coal panel. Int. J. Coal Geol. **71**, 313–328 (2007)

Zuber, M.D.: Production characteristics and reservoir analysis of coalbed methane reservoirs. Int. J. Coal Geol. **38**, 27–45 (1998)